

## Article

# Forecasting Live Fuel Moisture of *Adenostema fasciculatum* and Its Relationship to Regional Wildfire Dynamics across Southern California Shrublands

Isaac Park <sup>1,\*</sup>, Kristina Fauss <sup>2</sup> and Max A. Moritz <sup>3,4</sup>

<sup>1</sup> Department of Ecology, Evolution, and Marine Biology, University of California, Santa Barbara, CA 91336, USA

<sup>2</sup> Department of Geography, University of California, Santa Barbara, CA 91336, USA; kfauss@ucsb.edu

<sup>3</sup> University of California Cooperative Extension, Santa Barbara, CA 91336, USA; mmoritz@ucsb.edu

<sup>4</sup> Bren School of Environmental Science and Management, University of California, Santa Barbara, CA 91336, USA

\* Correspondence: isaac\_park@ucsb.edu

**Abstract:** In seasonally dry environments, the amount of water held in living plant tissue—live fuel moisture (LFM)—is central to vegetation flammability. LFM-driven changes in wildfire size and frequency are particularly important throughout southern California shrublands, which typically produce intense, rapidly spreading wildfires. However, the relationship between spatiotemporal variation in LFM and resulting long-term regional patterns in wildfire size and frequency within these shrublands is less understood. In this study, we demonstrated a novel method for forecasting the LFM of a critical fuel component throughout southern California chaparral, *Adenostema fasciculatum* (chamise) using gridded climate data. We then leveraged these forecasts to evaluate the historical relationships of LFM to wildfire size and frequency across chamise-dominant California shrublands. We determined that chamise LFM is strongly associated with fire extent, size, and frequency throughout southern California shrublands, and that LFM–wildfire relationships exhibit different thresholds across three distinct LFM domains. Additionally, the cumulative burned area and number of fires increased dramatically when LFM fell below 62%. These results demonstrate that LFM mediates multiple aspects of regional wildfire dynamics, and can be predicted with sufficient accuracy to capture these dynamics. Furthermore, we identified three distinct LFM ‘domains’ that were characterized by different frequencies of ignition and spread. These domains are broadly consistent with the management thresholds currently used in identifying periods of fire danger.

**Keywords:** fuel moisture; live fuel moisture; forecasting; climate; burned area



**Citation:** Park, I.; Fauss, K.; Moritz, M.A. Forecasting Live Fuel Moisture of *Adenostema fasciculatum* and Its Relationship to Regional Wildfire Dynamics across Southern California Shrublands. *Fire* **2022**, *5*, 110. <https://doi.org/10.3390/fire5040110>

Academic Editors: James A. Lutz and Alistair M. S. Smith

Received: 30 June 2022

Accepted: 20 July 2022

Published: 28 July 2022

**Publisher’s Note:** MDPI stays neutral with regard to jurisdictional claims in published maps and institutional affiliations.



**Copyright:** © 2022 by the authors. Licensee MDPI, Basel, Switzerland. This article is an open access article distributed under the terms and conditions of the Creative Commons Attribution (CC BY) license (<https://creativecommons.org/licenses/by/4.0/>).

## 1. Introduction

In seasonally dry environments around the world, the amount of water held in living plant tissue—live fuel moisture (LFM)—is central to both drought survival and flammability characteristics. Since the early research that linked LFM with actual fire occurrences in California [1–3] and Spain [4], studies have established relationships between LFM and wildfire across many ecosystems and regions, including southeastern Australia [5], central Argentina [6], and southwestern China [7]. A recent focus on LFM has even helped spawn the new sub-discipline of pyro-ecophysiology [8–11], which attempts to understand coincident drought and flammability traits. Across the world, collaborative efforts are now devoted to mapping LFM patterns in space and time [12]. Links between water stress (e.g., plant responses to avoid negative impacts) and characteristics of combustion (e.g., time to ignition, heat release) are clearly of growing interest. However, it remains unclear whether distinct stages of the fire season respond differently to variations in LFM.

LFM-driven changes in fire danger are particularly important throughout plant communities occupying Mediterranean-climates, which typically produce intense, stand-replacing fires that may spread rapidly [13]. These vegetation types also commonly occur along the wildland–urban interface (WUI) and in close proximity to human habitation, posing a significant threat to human life, structures, and essential infrastructure. Seasonal and interannual variations in LFM represent a major driver of this fire danger, as laboratory experiments have shown that fire spread is strongly linked to LFM among live chaparral fuel beds [14,15]. Similarly, the occurrence of fire in portions of coastal southern California has shown important linkages between LFM and the cumulative area burned, and has also exhibited critical thresholds of LFM, below which the burned area increases rapidly [3]. Findings obtained from other Mediterranean ecosystems [16] and even non-Mediterranean areas [6,7] also support the idea that there can be strong thresholds in the relationship between LFM and fire behavior, although the nature and location of thresholds may vary among vegetation types and among regions. Identifying links between LFM and resulting fire behavior, with particular emphasis on the location and strength of critical LFM thresholds in fire size and frequency, could thus be essential in forecasting fire danger in many fire-prone landscapes.

Although modeling and forecasting the LFM of critical fuel components is important for the prediction of local fire danger, spatially explicit forecasts of LFM and its relationship with wildfire risk have until recently remained limited. The moisture content of dead fuels can be easily modeled based on weather data [17,18]. However, the dynamics of live fuel moisture can be substantially more complex and difficult to model. Remote-sensing methods have been used successfully to determine historical patterns of spatiotemporal variation in LFM, but are limited to the time period for which remote sensing data is available, and cannot forecast future LFM [19,20]. Machine-learning [21] and statistical modelling approaches [22] have shown great promise in evaluating patterns of variation in LFM over space and time at broad spatial scales. However, the relationship between spatiotemporal variation in LFM and in resulting variations in regional wildfire dynamics remains unclear, as does the ability of such models to identify critical thresholds associated with changes in wildfire risk.

In this study, we examined novel methods for forecasting the LFM of *Adenostema fasciculatum* (also known as chamise), a shrub species representing a critical fuel component throughout southern California chaparral, as well as much of the southwestern United States. Chamise is a dual-rooted shrub that possesses both a shallow root system capable of capitalizing on winter rains, and a deep root system capable of tapping into subterranean water throughout the dry season when near-surface soil moisture is low and precipitation is unlikely [23–25]. The flammability of these fuels changes dramatically due to seasonal shifts in LFM, and previous examinations of the relationship between fire and seasonal LFM throughout Los Angeles County in California showed that fire activity increased sharply once LFM fell below ~79% [3]. Additionally, fires throughout chamise-dominated areas (see Materials and Methods) represent a major component of California fires, and chaparral-dominated areas account for a greater proportion of area burned throughout California than the proportion of the state they occupy. These attributes, alongside the high flammability and prevalence of chamise among chaparral ecosystems, make it an excellent candidate for LFM modeling efforts. However, the extensibility of these studies to broader regional vegetation and fire dynamics remains unclear. Furthermore, there is some question as to whether the observed thresholds in the relationship between burned area and LFM are due to increases in fire frequency when LFM falls below these thresholds (indicating more frequent and successful ignitions) or to increases in the sizes of individual fires [26].

To resolve these questions, we first modeled spatiotemporal variation in LFM within chamise-dominated areas, and then determined the precise relationship (and potential thresholds of these relationships) between LFM and wildfire. However, the observation of live fuel moisture is often spotty, with many spatial and temporal gaps in the observational

record. As a result, many fire events do not occur in close spatial or temporal proximity to in situ observations of LFM, making any attempt to determine the relationship between local LFM and fire problematic. This observational limitation typically restricts examinations of LFM–wildfire relationships to a relatively small number of fires, thereby limiting our ability to make inferences about the relationship of LFM to regional wildfire dynamics, which necessarily requires the evaluation of a large number of wildfire events. In this study, we resolved this limitation by modeling the relationship between local conditions and LFM over space and time, producing spatially and temporally explicit estimates of LFM for key fuel components across southern California chaparral. We then used these spatiotemporal estimates of LFM, in conjunction with in situ observations of LFM and records of past fire events, to evaluate the relationships of LFM with (a) cumulative burned area, (b) mean fire size, and (c) the cumulative number of fires.

## 2. Materials and Methods

### 2.1. Data Sets

All live fuel moisture data used in the model calibration were drawn from the National Fuel Moisture Database (NFMD, <https://www.wfas.net/nfmd/public/index.php> (accessed on 9 January 2020)), and these consisted of 19,639 individual observations of chamise fuel moisture across 61 sites throughout California, spanning the years 1977 through 2017. Climate data used in this study were drawn from the California Basin Characterization Model v8 [27], and consisted of monthly estimates of cumulative water deficit (CWD) and actual evapotranspiration (AET) measurements through the years 1951–2016. This dataset represents a 270 m grid-based model of water balance calculations that incorporates not only climate inputs (through PRISM climate data [28]) but also solar radiation, topographic shading, and cloudiness, along with soil properties to estimate evapotranspiration [29]. Using these monthly values, we calculated the mean maximum temperature (TMX), mean actual evapotranspiration (AET), mean climatic water deficit (CWD), mean precipitation (PPT), and mean soil moisture storage (STR) at 1, 6, and 12-month periods with lags of 1, 2, 3, 4, 5, and 6 months. Fire history data were drawn from FRAP fire perimeter data [30], which incorporate the perimeters of all known fires from 1878 through 2017. Vegetation data used to identify chamise vegetation in this study were drawn from both CALFIRE FRAP FVEG data [31] and the LANDFIRE 2016 Existing Vegetation Type (EVT) dataset [32].

### 2.2. Data Preparation

Observations of LFM were merged with data recording the latitude and longitude of each site and then filtered to exclude those observations not pertaining to chamise. As an LFM below 50 can represent dead material on the sampled shrubs, observed in situ estimates of LFM below 50% (which were exceedingly rare) were also excluded. Because LFM within each site was often recorded at inconsistent intervals that did not align with the monthly climate data used in this study, and many sites incorporated observations from multiple individual plants (the number of which also varied over time), we then calculated a single mean LFM within each month and site in which observations were present. In order to reduce the computational load to a manageable scale, all climate data were rescaled to 1 km pixels through spatial averaging, conducted using Rasterio in Python v3.7 [33]. Six-month and twelve-month mean TMX and total PPT, AET, CWD, and STR were then extracted at monthly timesteps using python v3.7.

### 2.3. Predicting Live Fuel Moisture across California

The most relevant climate parameters, lags, and window durations were identified by regressing each LFM observation against the corresponding monthly climate parameters (including TMX, PPT, AET, CWD, and STR) with lags of 1 to 6 months, as well as against the six-month means of each parameter over the six months preceding each observation. Overall relationships between chamise LFM and local climate at monthly timescales were

then modeled using a generalized additive model (GAM) framework. To minimize computational time while allowing for nonlinear relationships between local climate and LFM, a maximum of five smoothing terms was allowed for each climate parameter.

In order to determine the ability of this modeling technique to predict LFM in both (a) novel locations and (b) months not present in the training data, model performance was assessed using multidimensional k-fold cross-validation. All data were divided by month and year into to one of five randomly assigned temporal groups of equal size, and all were similarly divided into five randomly assigned spatial groups. GAM models were then constructed iteratively, while holding out one temporal and one spatial group as a testing data set within each iteration. The ability of these models to successfully predict LFM at monthly timescales was evaluated by calculating the mean Pearson correlation coefficient between the predicted LFM at training sites and months not used in model development, and the observed mean monthly LFM recorded at those sites and months across all model iterations. In order to avoid unnecessary complexity within these models and to limit the computational requirements, only parameters of which the inclusion increased the mean Pearson correlation coefficient by 0.02 or more were excluded from the selected model. In order to incorporate as long a wildfire series as possible, LFM was predicted monthly from 1952 through 2017.

#### *2.4. Identifying Fires of Interest*

First, we identified those fires in which chamise was likely to represent a major component of the overall fuel by eliminating those fires in which <50% of the burned area was predicted to consist of either Southern California coastal scrub or dry mesic chaparral according to the FVEG land cover dataset produced by CALFIRE-FRAP. Similarly, we eliminated all fires in which <50% of the burned area was predicted to consist of either mixed chaparral, chamise-redshanks chaparral, or coastal scrub according to EVT vegetation maps. Because of concerns surrounding mismatches among vegetation types between FVEG land cover data and EVT vegetation maps, only those fire scars which met both of these sets of criteria were selected for further analysis. It should be noted that these vegetation maps were static over time and did not attempt to incorporate variation in vegetation cover that may have occurred across the study period or immediately after disturbance events. However, annual assessments of vegetation cover throughout the study period were not available. Thus, although land cover may have fluctuated somewhat throughout the study period and immediately after fires or other disturbance events, these data nevertheless represented the best available data pertaining to the spatial distribution of chamise-dominated vegetation across California.

To evaluate the relationship of chamise LFM to the mean fire size, frequency, and cumulative area burned across southern Californian forests, it was first necessary to measure the predicted (and observed) LFM within the area burned during each fire. In order to summarize the predicted LFM within each fire at the time of ignition based on the gridded LFM estimates produced in this study, the mean predicted LFM in the month and year in which the initial ignition occurred was calculated across the entirety of each fire scar. The resulting data included 1818 individual fires from the year 1952 through 2017 (Figure 1).

#### *2.5. Identifying Critical Thresholds in LFM and Relationship to Burned Area*

To evaluate the relationship between LFM and fire, and to identify critical LFM thresholds associated with shifts in fire behavior, we first calculated the cumulative area burned with decreasing (simulated) LFM for all selected fire scars. As previous studies have shown that observed thresholds in LFM–wildfire relationships may be biased due to differences in the frequency with which different values of LFM occur over space and time [26], we converted these LFM values into percentile ranks based on the distribution of simulated LFM across the duration and spatial extent of this study. By carrying out this step, we corrected for any differences in the spatial or temporal frequency of LFM across the study area, which might otherwise bias the apparent relationships to cumulative

area burnt. Using these percentile LFM values, we then conducted piecewise or ‘broken stick’ regression [34] in order to identify transition points in LFM that were associated with an increasing burned area. After identifying thresholds in LFM–wildfire relationships using LFM percentiles, these percentile ranks could then be converted back into actual LFM values in order to identify the transition points in LFM–cumulative burned area relationships. Although similar analyses were conducted using in-situ observations of LFM, the sporadic spatiotemporal distribution of in-situ LFM observations precluded corrections for biases caused by differences in the frequency with which different values of LFM occur over space and time, and drastically reduced the number of fire events that for which LFM could be estimated. These limitations render interpretation or comparison to bias-corrected thresholds in LFM–wildfire relationships derived from gridded LFM data problematic, and are described in greater detail within the appendix (Figure A1).

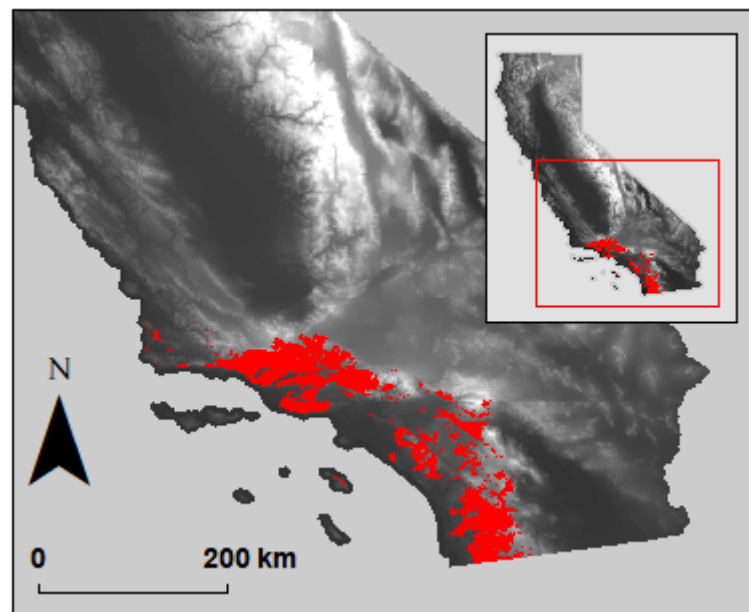


**Figure 1.** Study area, marked in red. The study area encompassed the 1818 fire scars examined in this study, which occurred from the year 1952 through 2017. Only fire scars in which  $\geq 50\%$  of the burned area consisted of either Southern California coastal scrub or dry mesic chaparral according to the FVEG land cover dataset produced by CALFIRE-FRAP, as well as  $\geq 50\%$  cover by mixed chaparral, chamise-redshanks chaparral, or coastal scrub according to EVT vegetation maps, were included.

## 2.6. Identifying Critical Thresholds in LFM and Relationship to Mean Fire Size

In order to determine whether the mean size of wildfires varied significantly with LFM, we similarly conducted piecewise analyses of the relationship between LFM and the mean size of all wildfires in which the predicted LFM (based on the mean LFM value across the burned area of each wildfire event) fell within a 5 percentile span (e.g., all fires in which LFM fell within the 5th to the 9.99th percentile). By evaluating mean fire size within set percentile ranges of LFM, this analysis eliminated any effects of differential fire frequency across the range of LFM, and enabled us to evaluate only the relationship of LFM to wildfire size. As with analyses of cumulative burned area, the identified percentile thresholds in LFM–wildfire relationships could then be converted back into actual LFM values in order to identify the actual transition points in LFM–mean-fire-size relationships.

## 2.7. Identifying Critical Thresholds in LFM and Relationship to Cumulative Number of Fires

Finally, in order to determine the degree to which low LFM was associated with a higher number of fires, and to identify critical thresholds of LFM below which fires occurred more frequently, we similarly conducted piecewise analyses of the relationship between

LFM percentile ranks and the cumulative number of fire events that had occurred. As with our analyses of the cumulative area burned, these analyses were conducted using LFM percentiles rather than raw LFM in order to compensate for potential differences in the spatial and temporal frequency of different ranges of LFM across the study area, and then converted post hoc data into actual LFM data in order to identify the actual threshold values. As percentile ranks of LFM inherently compensate for variable frequencies of different ranges of LFM values over space and time, the rates at which fires accumulate may be considered to be a measure of mean fire frequency within each range of LFM.

### 3. Results

GAM models successfully explained 65.4% of the observed variation in LFM among months, years, and locations not used in model development (Table 1, Figure 2). Furthermore, these models showed that cumulative precipitation over the preceding six months was the strongest predictor of LFM among chamise, followed by PPT and TMAX 2 months prior to observation (Figure 3). The mean absolute error (MAE) of these predictions was 11.46%, with a root mean squared error of 16.023. However, predictions were substantially more accurate during the dry season, in cases where LFM was low. When observed LFM was below 100%, MAE fell to 8.99%, whereas the MAE of the predicted LFM in locations and times where the observed LFM was 80% or less was only 8.33%.

**Table 1.** Parameters, lags, and  $R^2$  values of the selected GAM model. Individual  $R^2$  values indicate  $R^2$  values of GAM models which include only that parameter. Note that smoothing results for single-parameter models may be different from those of the multi-parameter model. Cumulative  $R^2$  values indicate  $R^2$  values of the model as parameters were added in stepwise fashion, and represent mean cross-validated  $R^2$  values among times and locations not used in model development. Cross validation was accomplished by dividing all data by month and year into to one of five randomly assigned temporal groups of equal size, and all were similarly divided into five randomly assigned spatial groups.

Parameter	Lag (Months)	Edf	Individual $R^2$	Cumulative $R^2$
6-Month PPT	0	3.985	0.538	0.538
Monthly PPT	2	2.978	0.490	0.633
Monthly TMAX	2	3.995	0.463	0.654

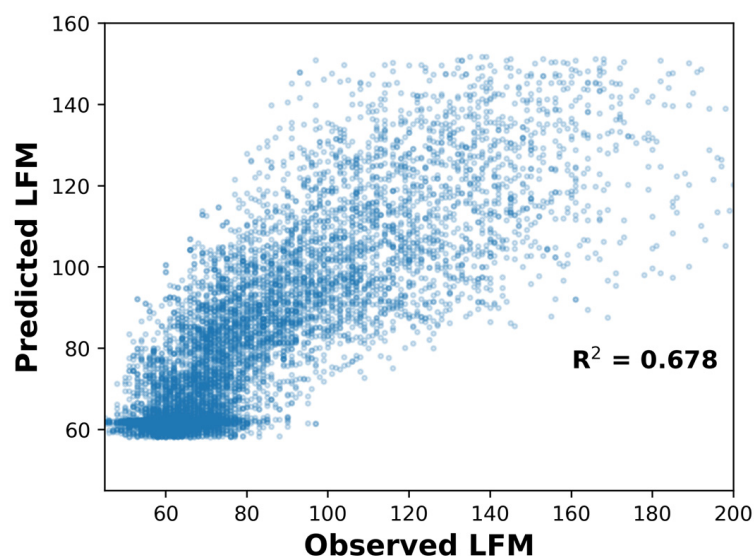


**Figure 2.** Predicted versus observed LFM of *Adenostema fasciculatum* (chamise) among all times and locations observed in this study.

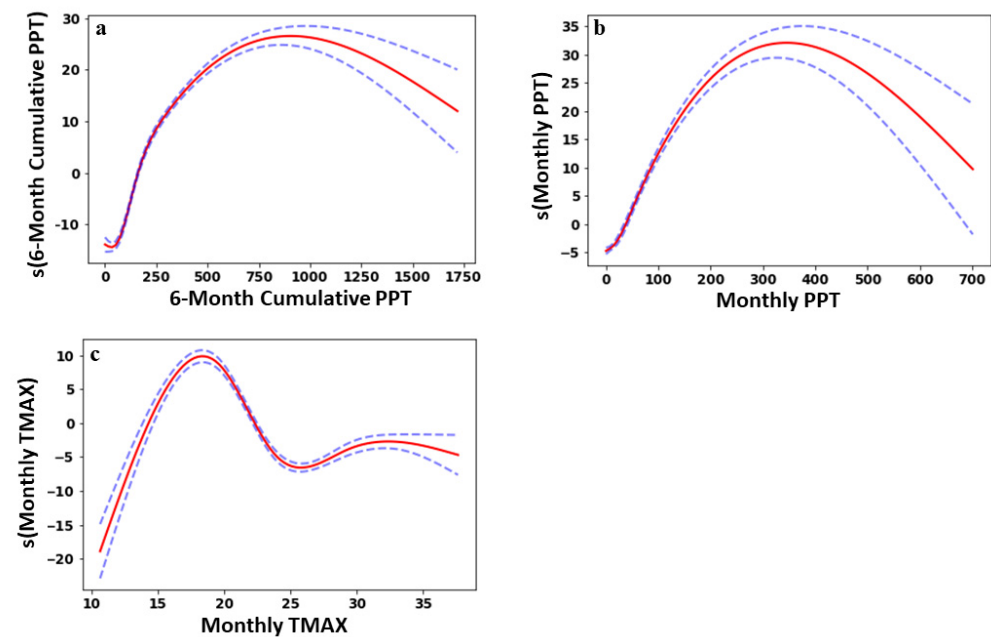


**Figure 3.** Smoothed coefficients of (a) cumulative precipitation over the prior six months, (b) monthly precipitation (2 month lag), and (c) mean maximum temperature (2 month lag) developed for GAM models used to predict LFM. Smoothed values ( $y$ -axis) represent contributions of each parameter to estimated LFM throughout the observed parameter space ( $x$ -axis). Solid red lines indicate smoothed coefficients. Dashed blue lines indicate 95% confidence intervals for each smoothed coefficient.

Both PPT and TMAX exhibited nonlinear relationships to LFM, with both 6 month and monthly lagged precipitation exhibiting strong positive relationships between PPT and LFM until reaching a saturation point, above which the relationship between precipitation and LFM were weakened and reversed. However, the sharp increases in the margins of error above these saturation points (roughly 800 mm in 6 month cumulative PPT and 350 mm in monthly PPT), implied a weak and nondeterministic relationship to LFM when PPT was high. In contrast, the relationship between LFM and TMAX remained strong throughout the entire observed temperature range, with low LFM predicted in association with low temperatures, reflecting winter dormancy, followed by high LFM predicted under temperatures ranging from approximately 25 to 22 °C, which likely reflected the peak growing season. TMAX showed minimal relationships with LFM above 25 °C, likely reflecting a reduced relationship between temperature and fuel moisture during the summer and autumn dry season when conditions are dry and transpiration is low regardless of temperature. Overall, these results would indicate that LFM during the dry season (corresponding to summer and autumn) is likely driven primarily by winter and spring precipitation, rather than by summer and fall temperatures.

### 3.1. LFM versus Cumulative Area Burned

Strong thresholds were detected in the relationship between cumulative burned area and live fuel moisture (Figure 4). Examinations of the relationship between cumulative burned area and simulated LFM identified two distinct thresholds in the relationship between cumulative burned area and simulated LFM (Figure 4). The burned area remained low while the simulated LFM remained above 76.9% (i.e., within the upper 57.7% of LFM values across the study area and period). However, the cumulative burned area was observed to increase rapidly with declining LFM once the simulated LFM fell below 76.9%, with an even sharper increase in the cumulative burned area once LFM fell below 61.1% (Figure 4). Notably, this indicates that approximately 40% of the total burned area occurred when LFM was below 61.1%, (in the lowest 8th percentile of LFM conditions), and approximately 80% of the burned area occurred under conditions within the lowest 42.3%

of LFM conditions. Although estimates of LFM thresholds calculated without adjustments to correct for the variable frequency of different LFM conditions across the study area did exhibit minor differences from these thresholds, threshold placement remained relatively similar (<5% change in both upper and lower thresholds, Figure A2a), and, in the case of the lower threshold, exhibited a much sharper transition in the cumulative burned area than was visible when examining LFM percentiles (Figure A2a).

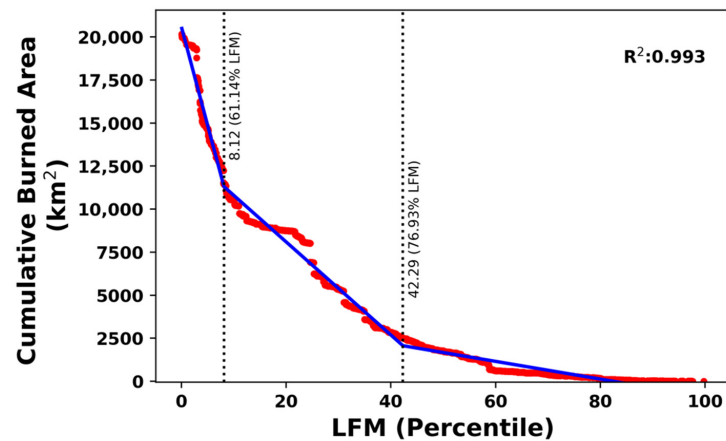


**Figure 4.** LFM of predicted LFM percentiles vs. cumulative area burned. Dashed lines indicate calculated locations of thresholds between LFM domains (measured both as LFM percentile rank and actual LFM).

### 3.2. LFM versus Mean Fire Size

As with cumulative burned area, mean fire size was observed to begin systematically increasing in association with lower LFM once LFM fell below 95.9% (representing the 67.4th percentile of LFM, Figure 5), and exhibited an even sharper relationship between increased fire size and reduced LFM as LFM fell below 62.1% (representing the 17.5th percentile of LFM across the study area, Figure 5). Thus, it appears that, independently of the number of fires that occurred across different LFM conditions, there was a strong relationship between reductions in LFM and increases in the average size of wildfires throughout the study area.

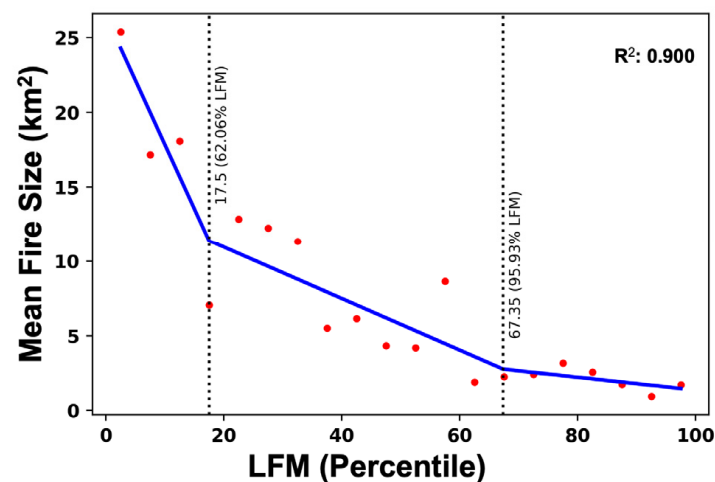


**Figure 5.** LFM of predicted LFM percentiles vs. mean fire size. Mean fire size was calculated as the mean area burned among all fires within each successive 5 percentiles of LFM. Dashed lines indicate calculated breakpoints between LFM domains (measured both as LFM percentile rank and actual LFM).

### 3.3. LFM versus Cumulative Number of Fires

As with the cumulative burned area, thresholds were detected in the relationship between the cumulative number of fire events and live fuel moisture (Figure 6). After correcting for the variable frequency of LFM conditions over space and time, the fire frequency was observed to increase when LFM dropped below 60.9% (representing the lowest 7.3% of observed LFM conditions over space and time). Similarly, the fire frequency was observed to be quite low when LFM rose above 89.0% (representing the 57.8th percentile of LFM conditions). Thus, the lower of these thresholds also remained similar to those observed in the relationship between simulated LFM and cumulative burned area (Figure 4), although the LFM threshold above which ignitions were less common appears to be higher than that observed in relation to cumulative burned area. Although estimates of LFM thresholds calculated without adjustments to correct for the variable frequency of different LFM conditions across the study area did exhibit minor differences from these thresholds, overall thresholds remained relatively similar (<5% change in both upper and lower thresholds, Figure A2b).

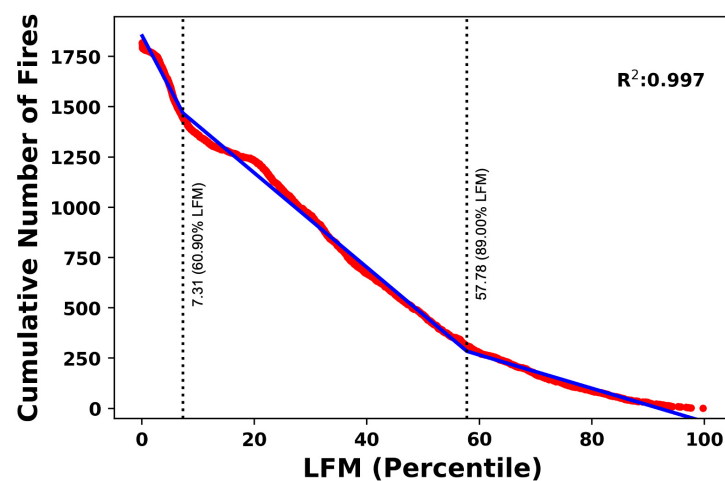


**Figure 6.** LFM of observed predicted LFM percentiles vs. cumulative number of fires. Dashed lines indicate calculated breakpoints between LFM domains (measured both as LFM percentile rank and actual LFM).

## 4. Discussion

This study demonstrated that the live fuel moisture of chamise can be predicted based on monthly climate data with a high degree of accuracy. As with previous examinations of chamise, antecedent precipitation appears to be the largest factor in determining LFM over space and time [3]. Predictions of LFM are also most accurate when in situ LFM is low, with more unexplained variance in LFM occurring when LFM is high (Figure 2). As fire risk is typically most sensitive to variations in LFM during the fire season when LFM is low [3] and is comparatively unaffected by variations in LFM during the wetter portions of the year, the observed model performance throughout the portion of the year when fire risks are high is likely much better than its overall performance across the entire range of conditions ( $R^2 = 0.654$ ,  $MAE = 11.46$ ,  $RMSE = 16.02$ , Figure 2). The modeled LFM produced in this study demonstrated similar predictive accuracy to remote-sensing based methods of forecasting LFM [19,35]. Unlike methods that depend on remote sensing data, however, this method relies solely on climate data, and can therefore be projected forward in time when future climate projections are available, or used to produce near-real-time estimates of LFM on the basis of local climate data in order to identify upcoming periods of high fire danger. Additionally, although the models presented here depend on precipitation and temperature (which were the best predictors of historical LFM across California), this framework can also be applied to model LFM directly based on gridded estimates of climatic water deficit (CWD) and actual evapotranspiration (AET). Although models utilizing these metrics

have exhibited mildly inferior predictive power to those driven solely by TMAX and PPT (Figures A3 and A4), they do provide a more mechanistic framework through which to understand the relationship of LFM to local conditions as experienced by plants. Thus, such models provide a unique opportunity to forecast LFM under projected future conditions (including possible non-analog future conditions which have no precedent in the historical record), in which estimates of temperature and precipitation may be less useful. Due to limitations in the temporal resolution of the climate data used in this study, these LFM predictions were limited to a monthly resolution. As in situ observations of LFM reflect the fuel moisture status of a plant on the day on which it was observed (which was then averaged across all observations in a given month), this may lead to some loss in predictive power in comparison to models developed with daily climate data [36]. However, the RMSE values of these monthly predictions were similar to those of daily predictions produced using more sophisticated models (RMSE = 16.023 in this study vs. RMSE = 15.34, as reported by Capps et al. [36]). Thus, these data were likely sufficient to evaluate broad trends in the relationships of LFM to burned area, wildfire size, and wildfire frequency across southern California shrublands.

We found that LFM plays an important role in the spatiotemporal distribution of fire at landscape to regional scales, supporting previous evidence that fire is more prevalent at times and locations in which LFM falls below certain thresholds [2,3,5,6]. Independently, the relationship observed here between LFM and the average size of wildfires (Figure 5) demonstrates that lower LFM is conducive to greater spread by individual fire events. These results confirm the findings of previous studies that showed the more rapid spread of fire among low-moisture fuels in laboratory experiments [14,37]. Furthermore, studies in the Chaco Serrano subregion of Argentina have also shown that high LFM often constrains the size of fire events [6], resulting in a greater frequency of large fires during periods of time when LFM is low. Similar patterns have also been found throughout Mediterranean shrublands, where low LFM among shrub species has been associated with a high burned area and greater frequency of large fires [4]. Thus, low LFM is strongly associated with both greater ignition success and the initial establishment of wildfire events (Figure 5), as well as a greater likelihood that each individual fire event will, once established, spread successfully to cover a wide area. It should be noted, however, that the thresholds identified in this study represent optimal breakpoints as identified through segmented regression, and do not necessarily imply sudden or drastic state changes in LFM–wildfire relationships. Instead, they should be interpreted as marking general transition points in the different phases of the fire season and in wildfire dynamics, as ignitability and fire spread rates change with progressively drier fuels. These dynamics will also likely be affected differently by local topography, fuel structure, microclimate, seasonal wind patterns, and many other factors that may affect the relationship of LFM with local wildfire dynamics [38,39]. Nevertheless, thresholds of dry fuel moisture have been implicated as the triggers for dynamic transformations of forest flammability across multiple continents and vegetation types [5,40]. Thus, as live fuel also makes up a significant component of the flammable material across the landscape, it is likely that the changes in LFM will also impact wildfire behavior.

Our finding of two thresholds in the relationship between simulated LFM and the burned area, mean fire size, and cumulative number of fires indicates that there are multiple domains of LFM–fire dynamics for this shrubland system. These findings support previous studies that identified multiple LFM–wildfire domains across both Europe and northern Africa [41]. The first domain represents conditions in which fuels are moist, and as a result, ignition rates are low, fire sizes remain small, and the cumulative burned area remains low. As fuels remain sufficiently hydrated as to limit both the ignition and spread of fire throughout this domain, changes in LFM within this domain appear to have only minimal effects on ignitability, fire size, and the rates at which the burned area increases. There is a wide range of variation in the LFM that limits this first domain (~77–96%) depending on which metric is being examined, indicating that this transition point is likely somewhat gradual, and may occur at slightly different LFM values depending on the aspect of

wildfire being measured. The second domain represents the range of LFM in which fuels become sufficiently dry for progressive reductions in LFM to impact ignitability and fire spread more strongly. Throughout this middle domain, progressive reductions in LFM appear to be associated with moderate increases in both ignitability and fire spread rates (as measured through examinations of mean fire size). However, these increases begin somewhat gradually in the upper portion of this domain, and only produce systematic increases in the rate of cumulative burned area accumulation throughout the lower half of this domain (when conditions range from ~62–77% LFM, Figures 4 and A2). The third and most distinct domain represents the driest conditions, in which any reduction in LFM results in dramatic increases both in ignitability (as measured via the cumulative number of fires) and fire size. This domain consists of conditions when LFM falls below ~62% and represents conditions in which fuel is extremely dry. In this domain, both fire frequency and size increase dramatically with reductions in LFM relative to conditions experiencing LFM values above this threshold, leading to rapid increases in the cumulative burned area, mean fire size, and fire frequency. In contrast to the transition between the first two (moister) LFM domains, which experienced a comparatively gradual transition in the relationships between LFM and ignitability and fire spread, this domain exhibits sudden, sharp increases in the cumulative number of fires, fire size, and cumulative burned area once LFM falls below ~62%, particularly when viewed in terms of actual LFM, rather than the LFM percentile (Figure A2). Thus, this lowest LFM threshold likely represents a critical indication of hazard for high fire conditions, as both fire frequency, mean fire size, and cumulative area burned were observed to increase sharply below this threshold.

Previous examinations of LFM in Los Angeles county identified only a single sharp threshold in the relationship between the LFM of chamise and the cumulative burned area [3], which occurred at 79% LFM. This observed threshold coincides with the observed threshold between the wettest and middle domains in the LFM–burned-area relationship (at 77% LFM) that was observed in this study, although examinations of the relationships between LFM and mean fire size or cumulative number of fires exhibited some variation in the placement of this threshold (77–96% LFM). The sharpest and most consistent threshold observed in this study, however, occurred under much drier conditions, at ~61–62% LFM, representing the transition point into the third and driest domain observed in this study. This lower threshold also corresponds to the perceived LFM thresholds often used by firefighters to determine local fire danger throughout southern California [15]. Previous examinations of fire size distributions have also showed that fire sizes across many California ecosystems exhibit a three-domain distribution, which supports the results of this study [42]. These findings also indicate that LFM may be the driver (or one of the primary drivers) in generating such a distribution of fire sizes. Inconsistencies in the upper LFM threshold (~77–95%) may be partially due to the greater error in predictions of LFM during conditions when fuel moisture is increasingly wet, and may also represent a more gradual transition between the wettest and middle LFM domains. Additionally, some aspects of differences in LFM–wildfire relationships among these domains may be influenced by seasonal differences in wind and the confluence between the timing of progressive reductions in LFM and the occurrence of Santa Ana winds and other extreme events that are closely associated with extreme fire sizes and rapid fire spreads [43]. As LFM predictions in this study were driven by local climate conditions, as well as many effects of long-term climate shifts (such as increasing temperatures or drought conditions) that may have occurred across the study period should be reflected in predicted LFM values, it should also be noted that this study does not explicitly account for any potential non-stationarities across the study period that may have resulted from changes in land use or anthropogenic ignition rates. Thus, despite the strong concurrence observed with commonly used LFM thresholds based on expert information [15], it is not yet known how generalizable our findings are to other regions or vegetation types.

## 5. Conclusions

In this study, we demonstrated that LFM impacts wildfire throughout southern California through multiple mechanisms, by altering both the frequency of wildfire events and the probability that small wildfire events will expand to become larger fires. We also identified three distinct domains in the relationship between wildfires and LFM, and identifies consistent thresholds in the relationship between LFM and wildfire behavior that are consistent with the management thresholds used by firefighters in identifying periods of high fire danger. Furthermore, we have demonstrated a novel methodology for estimating LFM that is capable not only of predicting in situ LFM with a high degree of accuracy over space and time, but of capturing broad patterns in the spatiotemporal distribution of wildfire across chaparral in Southern California. As these methods advance and additional data become available, such techniques may be expanded to accommodate a wider array of plant taxa that represent major fuel components throughout the western United States. In particular, our goal is to further examine the effects of historical and projected changes in climate on LFM, to identify whether the three domains found in this study are representative of fire regimes across other vegetation types and climate regimes.

**Author Contributions:** Conceptualization, I.P. and M.A.M.; methodology, I.P., K.F. and M.A.M.; software, I.P. and K.F.; validation, I.P. and K.F.; formal analysis, I.P. and K.F.; data curation, I.P. and K.F.; writing—original draft preparation, I.P.; writing—review and editing, I.P. and M.A.M.; funding acquisition, M.A.M. All authors have read and agreed to the published version of the manuscript.

**Funding:** This research was funded by the University of California’s National Laboratories (UCNL) Laboratory Fees grant program under grant number LFR-18-542511 (as a part of the California Ecosystems Futures project), as well as by the California Department of Forestry and Fire Protection, Fire and Resource Assessment Program (CAL FIRE—FRAP, <https://frap.fire.ca.gov/>) and California Climate Investments, under CAL FIRE contract numbers 8CA03698 and 8GG20803.

**Informed Consent Statement:** Not applicable.

**Data Availability Statement:** Fuel moisture data used in this study are publicly available through the National Fuel Moisture Database (<https://www.wfas.net/nfmd/public/index.php> (accessed on 9 January 2020)). Climate data used in this study are publicly available through the United States Geological Survey (<https://www.sciencebase.gov/catalog/item/5f29c62d82cef313ed9edb39> (accessed on 5 January 2019)). All code pertaining to the analyses conducted in this study are available through DRYAD (<https://doi.org/10.25349/D9HS51>).

**Acknowledgments:** We would like to acknowledge Allan Flint and Lorraine Flint for assistance in acquiring and processing the climate data used in this study.

**Conflicts of Interest:** The funders had no role in the design of the study; in the collection, analyses, or interpretation of data; in the writing of the manuscript, or in the decision to publish the results.

## Appendix A

To examine the relationships between fire and observed LFM, we included all fires located within a 20 km site in which chamise was observed in the same month and year as the ignition of the fire. This method parallels a previously established methodology used to evaluate the relationship between LFM and cumulative area burned throughout the Santa Monica mountains in southern California [3]. The resulting data included 353 individual fires (Figure 1) from the years 1952 through 2017. It should be noted, however, that thresholds in LFM–burned-area relationships obtained using these data cannot be corrected in regard to the differing frequency of LFM conditions over space and time, and are therefore not equivalent to the thresholds calculated using simulated LFM. Furthermore, in these analyses we utilized only 353 fire events, rather than the 18,18 fires available for the analysis of simulated LFM. However, these analyses are presented here for comparison, and to demonstrate that despite their restricted sample size and the inability to compensate for the variable frequency of LFM conditions, broad similarities do exist in the LFM–burned-area and LFM–fire-frequency relationships derived using these data and those derived

from simulated LFM. Due to the limited number of fires for which in situ observations of LFM were available, however, comparisons of the relationship between LFM and mean fire size were not appropriate.

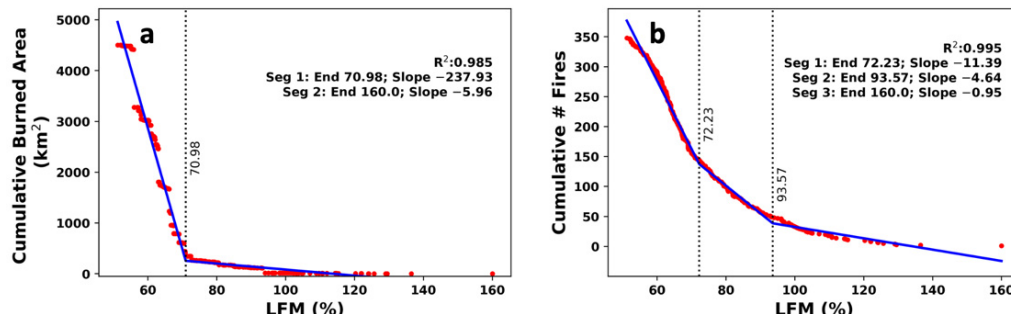


Figure A1. LFM of (a) observed in situ LFM v. cumulative burned area, and (b) observed in situ LFM vs. cumulative number of fires.

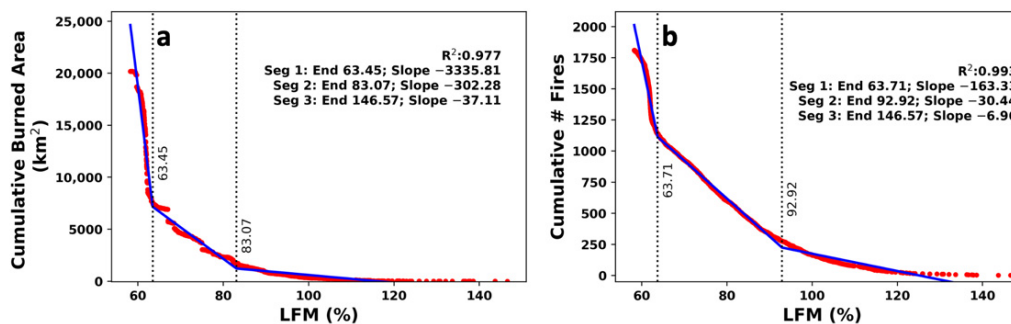


Figure A2. LFM of (a) predicted LFM v. cumulative burned area, and (b) predicted LFM vs. cumulative number of fires. Breakpoints were calculated based solely on the observed mean LFM within the recorded wildfire perimeters, and were not adjusted to correct for the variable frequency of LFM over space or time.

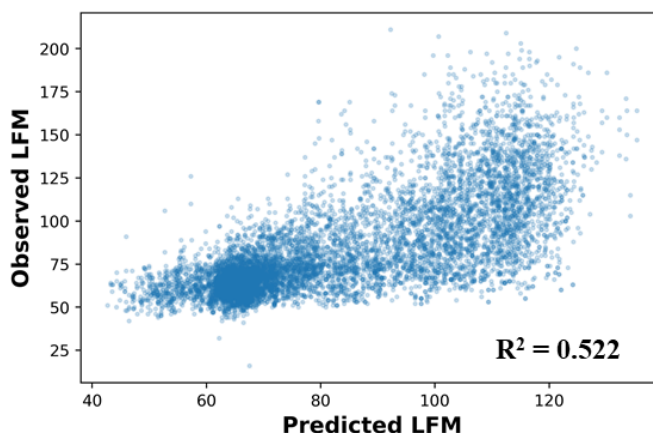
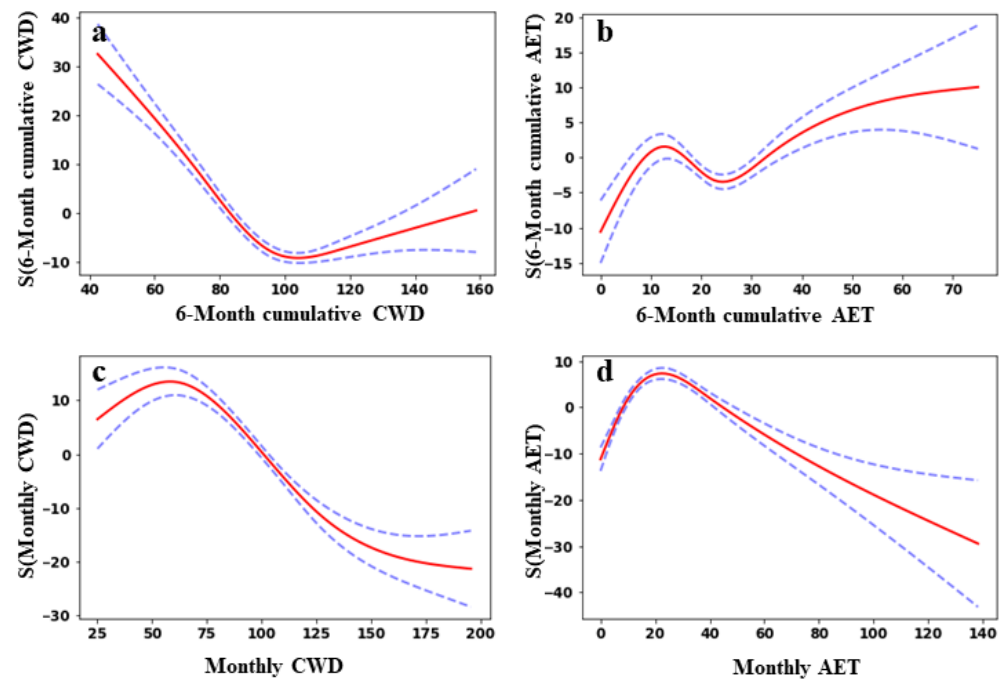


Figure A3. Predicted versus observed LFM of *Adenostema fasciculatum* (chamise) among all times and locations observed in this study, using a model calculated based on 6 month cumulative CWD, and 1 month CWD and AET (with lags of 2 months).



**Figure A4.** Smoothed coefficients of (a) cumulative precipitation over the prior six months, (b) monthly precipitation (2 month lag), (c) mean maximum temperature (2 month lag), and (c,d) mean monthly precipitation (2 month lag).

## References

- Schoenberg, F.P.; Peng, R.; Huang, Z.; Rundel, P. Detection of non-linearities in the dependence of burn area on fuel age and climatic variables. *Int. J. Wildland Fire* **2003**, *12*, 1–6. [\[CrossRef\]](#)
- Dennison, P.E.; Moritz, M.A.; Taylor, R.S. Evaluating models of critical live fuel moisture in the Santa Monica Mountains, California. *Int. J. Wildland Fire* **2008**, *17*, 18–27. [\[CrossRef\]](#)
- Dennison, P.E.; Moritz, M.A. Critical live fuel moisture in chaparral ecosystems: A threshold for fire activity and its relationship to antecedent precipitation. *Int. J. Wildland Fire* **2009**, *18*, 1021–1027. [\[CrossRef\]](#)
- Chuvieco, E.; González, I.; Verdú, F.; Aguado, I.; Yebra, M. Prediction of fire occurrence from live fuel moisture content measurements in a Mediterranean ecosystem. *Int. J. Wildland Fire* **2009**, *18*, 430–441. [\[CrossRef\]](#)
- Nolan, R.H.; Boer, M.M.; de Dios, V.R.; Caccamo, G.; Bradstock, R.A. Large-scale, dynamic transformations in fuel moisture drive wildfire activity across southeastern Australia. *Geophys. Res. Lett.* **2016**, *43*, 4229–4238. [\[CrossRef\]](#)
- Argañaraz, J.P.; Landi, M.A.; Scavuzzo, C.M.; Bellis, L.M. Determining fuel moisture thresholds to assess wildfire hazard: A contribution to an operational early warning system. *PLoS ONE* **2018**, *13*, e0204889. [\[CrossRef\]](#)
- Luo, K.; Quan, X.; He, B.; Yebra, M. Effects of live fuel moisture content on wildfire occurrence in fire-prone regions over southwest China. *Forests* **2019**, *10*, 887. [\[CrossRef\]](#)
- Jolly, W.M.; Johnson, D.M. Pyro-ecophysiology: Shifting the paradigm of live wildland fire research. *Fire* **2018**, *1*, 8. [\[CrossRef\]](#)
- Nolan, R.H.; Hedo, J.; Arteaga, C.; Sugai, T.; de Dios, V.R. Physiological drought responses improve predictions of live fuel moisture dynamics in a Mediterranean forest. *Agric. For. Meteorol.* **2018**, *263*, 417–427. [\[CrossRef\]](#)
- Pivovarov, A.L.; Emery, N.; Sharifi, M.R.; Witter, M.; Keeley, J.E.; Rundel, P.W. The Effect of Ecophysiological Traits on Live Fuel Moisture Content. *Fire* **2019**, *2*, 28. [\[CrossRef\]](#)
- Nolan, R.H.; Blackman, C.J.; De Dios, V.R.; Choat, B.; Medlyn, B.E.; Li, X.; Bradstock, R.A.; Boer, M.M. Linking forest flammability and plant vulnerability to drought. *Forests* **2020**, *11*, 779. [\[CrossRef\]](#)
- Yebra, M.; Scortechini, G.; Badi, A.; Beget, M.E.; Boer, M.M.; Bradstock, R.; Chuvieco, E.; Danson, F.M.; Dennison, P.; de Dios, V.R.; et al. Globe-LFMC, a global plant water status database for vegetation ecophysiology and wildfire applications. *Sci. Data* **2019**, *6*, 155. [\[CrossRef\]](#)
- Keeley, J.E.; Bond, W.J.; Bradstock, R.A.; Pausas, J.G.; Rundel, P.W. *Fire in Mediterranean Ecosystems: Ecology, Evolution and Management*; Cambridge University Press: Cambridge, UK, 2011.
- Zhou, X.; Weise, D.; Mahalingam, S. Experimental measurements and numerical modeling of marginal burning in live chaparral fuel beds. *Proc. Combust. Inst.* **2005**, *30*, 2287–2294. [\[CrossRef\]](#)
- Weise, D.R.; Zhou, X.; Sun, L.; Mahalingam, S. Fire spread in chaparral—‘Go or no-go?’. *Int. J. Wildland Fire* **2005**, *14*, 99–106. [\[CrossRef\]](#)

16. Dimitrakopoulos, A.P.; Papaioannou, K.K. Flammability Assessment of Mediterranean Forest Fuels. *Fire Technol.* **2001**, *37*, 143–152. [[CrossRef](#)]
17. Nolan, R.H.; Resco de Dios, V.; Boer, M.M.; Caccamo, G.; Goulden, M.L.; Bradstock, R.A. Predicting dead fine fuel moisture at regional scales using vapour pressure deficit from MODIS and gridded weather data. *Remote Sens. Environ.* **2016**, *174*, 100–108. [[CrossRef](#)]
18. Matthews, S. Dead fuel moisture research: 1991–2012. *Int. J. Wildland Fire* **2014**, *23*, 78–92. [[CrossRef](#)]
19. Fan, L.; Wigneron, J.P.; Xiao, Q.; Al-Yaari, A.; Wen, J.; Martin-StPaul, N.; Dupuy, J.L.; Pimont, F.; Al Bitar, A.; Fernandez-Moran, R.; et al. Evaluation of microwave remote sensing for monitoring live fuel moisture content in the Mediterranean region. *Remote Sens. Environ.* **2018**, *205*, 210–223. [[CrossRef](#)]
20. Zhu, L.; Webb, G.I.; Yebra, M.; Scortechini, G.; Miller, L. Live fuel moisture content estimation from MODIS: A deep learning approach. *ISPRS J. Photogramm. Remote Sens.* **2021**, *179*, 81–91. [[CrossRef](#)]
21. Littell, J.S.; Gwozdz, R.B. Climatic Water Balance and Regional Fire Years in the Pacific Northwest, USA: Linking Regional Climate and Fire at Landscape Scales. In *The Landscape Ecology of Fire*; McKenzie, D., Miller, C., Falk, D.A., Eds.; Springer: Dordrecht, Netherlands, 2011; pp. 117–139.
22. Vinodkumar, V.; Dharssi, I.; Yebra, M.; Fox-Hughes, P. Continental-scale prediction of live fuel moisture content using soil moisture information. *Agric. For. Meteorol.* **2021**, *307*, 108503. [[CrossRef](#)]
23. Lambers, H.; Chapin, F.; Pons, T. *Plant Physiological Ecology*; Springer: New York, NY, USA, 2008.
24. Helmers, H.; Horton, J.; Juhren, G.; O'keefe, J. Root systems of some chaparral plants in Southern California. *Ecology* **1955**, *36*, 667–678. [[CrossRef](#)]
25. Henson, P.; Usner, D.; Kells, V. *The Natural History of Big Sur*; University of California Press: California, CA, USA, 1996.
26. Pimont, F.; Ruffault, J.; Martin-StPaul, N.K.; Dupuy, J.-L. A Cautionary Note Regarding the Use of Cumulative Burnt Areas for the Determination of Fire Danger Index Breakpoints. *Int. J. Wildland Fire* **2019**, *28*, 254–258. [[CrossRef](#)]
27. Flint, L.E.; Flint, A.L.; Stern, M.A. The Basin Characterization Model version 8—A Regional Water Balance Code Calibration and Application. *U.S. Geol. Surv. Tech. Methods* **2021**, in press.
28. Group, P.C. PRISM Climate Group; Corvallis, OR, USA; 2004. Available online: <http://prism.oregonstate.edu> (accessed on 5 January 2020).
29. Flint, L.; Flint, A.; Thorne, J.; Boynton, T. *California Basin Characterization Model Downscaled Climate and Hydrology*; USGS: Reston, VA, USA, 2013.
30. FRAP. *Fire Perimeter Project Introduction*; The Fire and Resource Assessment Program (FRAP): Santa Barbara, CA, USA, 2019.
31. California Department of Forestry and Fire Protection. *Vegetation (fveg)—CALFIRE FRAP [ds1327] SDE Raster Dataset*; California Natural Resources Agency: Santa Barbara, CA, USA, 2015.
32. *LANDFIRE Remap 2016 National Vegetation Classification (NVC) CONUS*; USGS: Reston, VA, USA, 2020.
33. Van Rossum, G.; Drake, F.L. *Python 3 Reference Manual*; CreateSpace: Scotts Valley, CA, USA, 2009.
34. Toms, J.D.; Lesperance, M.L. Piecewise regression: A tool for identifying ecological thresholds. *Ecology* **2003**, *84*, 2034–2041. [[CrossRef](#)]
35. Tanase, M.A.; Panciera, R.; Lowell, K.; Aponte, C. Monitoring live fuel moisture in semiarid environments using L-band radar data. *Int. J. Wildland Fire* **2015**, *24*, 560–572. [[CrossRef](#)]
36. Capps, S.B.; Zhuang, W.; Liu, R.; Rolinski, T.; Qu, X. Modelling chamise fuel moisture content across California: A machine learning approach. *Int. J. Wildland Fire* **2022**, *31*, 136–148. [[CrossRef](#)]
37. Rossa, C.G.; Veloso, R.; Fernandes, P.M. A laboratory-based quantification of the effect of live fuel moisture content on fire spread rate. *Int. J. Wildland Fire* **2016**, *25*, 569–573. [[CrossRef](#)]
38. Brown, T.P.; Inbar, A.; Duff, T.J.; Burton, J.; Noske, P.J.; Lane, P.N.J.; Sheridan, G.J. Forest structure driven fuel moisture response across alternative forest states. *Fire* **2021**, *4*, fire4030048. [[CrossRef](#)]
39. Weise, D.R.; Koo, E.; Zhnou, X.; Mahalingam, S.; Marandini, F.; Balbi, J.-H. Fire spread in chaparral—A comparison of laboratory data and model predictions in burning live fuels. *Int. J. Wildland Fire* **2016**, *25*, 980–994. [[CrossRef](#)]
40. Boer, M.M.; Nolan, R.H.; Resco De Dios, V.; Clarke, H.; Price, O.F.; Bradstock, R.A. Changing Weather Extremes Call for Early Warning of Potential for Catastrophic Fire. *Earth's Future* **2017**, *5*, 1196–1202. [[CrossRef](#)]
41. Loepfe, L.; Rodrigo, A.; Lloret, F. Two thresholds determine climatic control of forest fire size in Europe and northern Africa. *Reg. Environ. Change* **2014**, *14*, 1395–1404. [[CrossRef](#)]
42. Moritz, M.A.; Hessburg, P.F.; Povak, N.A. Native fire regimes and landscape resilience. In *The Landscape Ecology of Fire*; McKenzie, D., Miller, C., Falk, D.A., Eds.; Springer: New York, NY, USA, 2011.
43. Moritz, M.A.; Moody, M.A.; Krawchuk, M.A.; Hughes, M.; Hall, A. Spatial variation in extreme winds predicts large wildfire locations in chaparral ecosystems. *Geophys. Res. Lett.* **2010**, *37*, L04801. [[CrossRef](#)]